Desalination and Water Treatment
www.deswater.com

doi: 10.1080/19443994.2016.1166396

57 (2016) 26401–26413
November

Taylor & Francis
Taylor & Francis Group

Comparison of different modified aluminosilicate networks for the removal of diclofenac

P.A. Gamboa[a], J.J. Ramírez-García[a,*], M. Solache-Ríos[b], C. Díaz-Nava[c], J.L. Gallegos-Pérez[d]

[a]*Facultad de Química, Universidad Autónoma del Estado de México, Paseo Colón esq, Paseo Tollocan, Toluca, Estado de México C.P. 50120, México, email:* pags_17@hotmail.com *(P.A. Gamboa), Tel./Fax: +52 722 2 17 3890; email:* jjramirezg@uaemex.mx *(J.J. Ramírez-García)*

[b]*Departamento de Química, Instituto Nacional de Investigaciones Nucleares, A.P. 18-1027, Col. Escandón, Delegación Miguel Hidalgo, DF C.P 11801, México, email:* marcos.solache@inin.gob.mx

[c]*Instituto Tecnológico de Toluca, División de Estudios de Posgrado, Av. Tecnológico s/n, Ex Rancho La Virgen, Metepec, Estado de México C.P. 52140, México, email:* mdiazn@ittoluca.edu.mx

[d]*Laboratory Neurobiology and Behavior Department, University of California Irvine, 2205 McGaugh Hall, Irvine, CA 92697, USA, email:* joseluis.gallegos@sciex.com

Received 5 November 2015; Accepted 3 March 2016

ABSTRACT

Different modified hexadecyltrimethylammonium (HDTMA) aluminosilicate networks were used to remove diclofenac (DS) from aqueous solutions, in order to know how important the networks of the aluminosilicates in adsorption processes are. HDTMA modified zeolitic tuff and HDTMA modified clay samples were characterized by X-ray Diffraction, Thermal Gravimetric Analysis, Fourier Transform Infrared Spectroscopy, and Scanning Electron Microscopy. The adsorption kinetics data were described by the pseudo-second-order kinetic model, and the Langmuir model described the isotherm of DS by the HDTMA modified zeolitic tuff (SMZ-25 and SMZ-50) which indicated chemical adsorption on homogeneous materials. The equilibrium isotherms for HDTMA modified clay (SMC-50) followed a linear behavior which is characteristic of sorption of organic solutes sorption by the partition mechanism. The maximum sorption capacities were 0.826 ± 0.004 mg/g for SMZ-25 and 0.880 ± 0.012 mg/g for SMC-50. According to the kinetic and isotherm results, SMZ-25 and SMC-50 showed the best properties to remove DS from aqueous solutions.

Keywords: Clinoptilolite; Montmorillonite; Diclofenac; Cationic surfactant; Drug sorption

---

1. Introduction

In the last decades, the use of pharmaceuticals in human and veterinary medicine has increased considerably. Pharmaceutically active compounds (PACs) are usually soluble in water because they are often polar molecules and they are not completely metabolized. Consequently, PACs together with the products of metabolization are excreted through urine or feces and enter in wastewaters as biologically active substances [1–3].

Diclofenac (DS) is one of the most frequently detected pharmaceutical in aquatic environments [4]; this is a nonsteroidal anti-inflammatory drug commonly used for the treatment of arthritis [5], it can also be used to reduce menstrual pain. The concentration of pharmaceuticals detected in the

---

*Corresponding author.

environment is quite low (96–510 ng/L) [6]. The ecotoxicology by pharmaceuticals at μg/L levels have been reported [7].

The impact of DS has been evaluated in some systems like: carbamazepine and DS in bacteria, algae, microcrustaceans, and fish, the concentrations that cause 50% of effect (EC50) were 13,800 μg/L for carbamazepine on *D. magna* over 48 h and 11,454 μg/L for DS on the Microtox® system over 30 min [7], The lethal concentration in zebra fish embryos is 5,900 μg/L [8]; alterations in the kidney and gills were found in rainbow trout (*Oncorhynchus mykiss*) exposed to DS (1–500 μg/L) for a period of 28 d found [9].

Different methods have been reported to remove organic contaminants from water, such as nanofiltration [10], reverse osmosis [11], ozonation [12], chemical oxidation [13,14], and adsorption [15,16]. Inorganic adsorbents offer advantages, due to their stability toward radioactive and thermal treatments. Modified aluminosilicates such as zeolites are efficient to remove some organic compounds from the environmental [17].

Zeolites have the ability to lose and gain water reversibly; they adsorb molecules of appropriate diameter and exchange inorganic cations. They are hydrated microporous tectoalumosilicates consisting of frameworks of SiO_4 and AlO_4 tetrahedra linked through shared oxygen atoms. The partial substitution of Al^{3+} for Si^{4+} results in an excess of negative charge which is compensated by alkali and earth alkaline cations [18].

Clays are ionic exchanger as zeolites; the montmorillonite surface is hydrophilic in nature due to hydration of inorganic cations on the exchange sites and they may be modified with surfactants. Quaternary ammonium cations have been used to modify aluminosilicates; the gap between the single sheets is widened, enabling organic cation chains to move between them, and the surface properties of each single sheet are changed from being hydrophilic to hydrophobic [19]. Redding et al. [20] reported that a modified clay sorbs organic contaminants through adsorption or partitioning phenomenon.

There are a few papers in the literature on the removal of DS by aluminosilicates. Some adsorbents used for DS removal from aqueous solution are: surfactant-modified zeolites tuffs [21], hexagonal mesoporous silicate [5], mesoporous silica SBA-15 [22].

The objective of this research was to determine the effect of different aluminosilicate networks on the removal of DS from aqueous solutions by using hexadecyltrimethylammonium (HDTMA) modified aluminosilicates (clinoptilolite and montmorillonite).

2. Experimental

2.1. Chemicals

Reagents-grade chemicals were used as received without further purification. A clinoptilolite-rich zeolitic tuff (Z) was obtained from Tehuacán, Mexico. The mineral was extracted as crushed rock aggregate. It was milled and sieved to a grain size between 0.840 and 0.420 mm and the sodium commercial montmorillonite clay (C-Na) was obtained from Veracruz, México it was milled and sieved to obtain particle sizes between 0.177 and 0.124 mm.

Technical grade (99% purity) DS was purchased from Sigma Aldrich, HLPC grade acetonitrile (ACN) and formic acid (analytical reagent grade, 88%) were from Fermont and water was Milli-Q grade.

2.2. Sodium modified zeolitic tuff (Z-Na)

One hundred grams of Z were treated with 1 L of 0.1 M NaCl solution, the mixture was refluxed for 3 h, the phases were separated, and this procedure was repeated twice. Finally, the zeolitic sample was washed with deionized water until chloride ions were not detected in the washing solution using a $AgNO_3$ test. Finally, the Z-Na was dried at room temperature for 24 h [23].

2.3. HDTMA modified zeolitic tuff and clay

Samples of 25 g of the Z-Na or C-Na were left in contact with 250 mL of 25 or 50 mmol/L HDTMA bromide solutions for 48 h, 30˚C, and 100 rpm. Then, the solids were washed 31 times with deionized water at room temperature to eliminate the excess of surfactant on the materials (until the surfactant was not observed in the washing solution by a UV–vis Lambda 25 Perkin Elmer spectrophotometer at 219 nm). The modified samples were labeled as SMZ-25 and SMZ-50 for the HDTMA modified zeolitic tuff and SMC-25 and SMC-50 for the HDTMA modified clay.

2.4. Zero Charge Point (ZCP)

Zero charge points were determined for Z-Na, C-Na, and HDTMA modified zeolitic tuffs and clays, the experiments were performed as follows: 0.1 M $NaNO_2$ solution of pH values between 1 and 11, with intervals of 1 unit (adjusted by adding 0.1 M HCl or NaOH solutions) were left in contact with each material. After 24 h of contact at 25˚C and 100 rpm, the clay mixtures were centrifuged and decanted, the zeolitic tuff mixtures were decanted, and pH was analyzed in the final liquid phases with an equipment Standard pH Meter model pHM210 [24].

2.5. High performance liquid chromatography (HPLC) analysis

The chromatographic system Waters consisted of an isocratic High performance liquid chromatography (HPLC) Pump and a UV–vis Dual Absorbance Detector. Separations were performed using an Eclipse XDB-C_{18} 4.6 × 250 mm, 5 μm particle column. A sample volume of 20 μL was injected through a loop. Flow rate of the mobile phase was 1 mL/min; UV detection was performed at 267 nm. The analysis was performed using ACN as eluent A and HPLC grade water with 0.1% formic acid as eluent B (70:30, v/v). The experiments were performed in duplicate.

2.6. Kinetics

One hundred milligram samples of Z, SMZ-25, SMZ-50, C-Na, SMC-25, and SMC-50 were put in contact with 10 mL of DS solution (10 mg/L). The mixtures were shaken for different times (15, 30, and 45 min and 1, 3, 6, 9, 12, 15, 18, 21, 24, 28, 32, 36, 40, 44, 48, 54, 60, 66, and 72 h) at 25˚C, then the clay mixtures were centrifuged and the zeolitic tuff mixtures decanted. The initial and final concentrations of DS were determined by HPLC analysis as described above.

The sorption behavior was analyzed by using nonlinear models.

2.6.1. Pseudo-first-order model (Lagergren)

Lagergren first-order model [25] is represented by the following equation:

$$q_t = q_{\mathrm{e}}^{(1-\exp(-K_{\mathrm{L}}))} \tag{1}$$

where q_t (mg/g) is the amount of DS adsorbed at time t, q_{e} (mg/g) is the amount of DS adsorbed at equilibrium, and K_{L}/h is the Lagergren rate constant.

2.6.2. Second-order model (Elovich)

The Elovich rate model equation has been used in the kinetics of chemisorption of gasses on solids. However, some researchers have applied this model to solid–liquid sorption systems [26].

This model is represented by the following equation:

$$q_t = 1/\beta \ \ln\,(1 + \alpha\beta t) \tag{2}$$

where q_t (mg/g) is the amount of DS adsorbed at time t, α (mg/g h) is the sorption constant of the DS, and β (g/mg) is the desorption constant of the DS.

Elovich equation was simplified assuming $\alpha\beta t >> 1$ and by applying the boundary conditions $q_t = 0$ at $t = 0$ and $q_t = q_t$ at $t = t$ and Eq. (2) becomes:

$$q_t = \beta \ \ln(\alpha\beta) + \ln(t) \tag{3}$$

2.6.3. Pseudo-second-order model

The nonlinear form of the pseudo-second-order model [26] can be represented by the following equation:

$$q_t = Kq_{\mathrm{e}}^2 t/(1 + Kq_{\mathrm{e}}t) \tag{4}$$

where K (g/mg h) is the constant of pseudo-second-order, q_t (mg/g) is the amount of DS adsorbed at time t, and q_{e} (mg/g) is the amount of DS adsorbed at equilibrium.

The pseudo-second-order model is based on the assumption that the rate limiting step may be the process of chemisorption involving valence forces through sharing or exchange of electrons between sorbent and sorbate [27].

2.7. Isotherms

According to the kinetic results, SMC-25 showed low adsorption efficiency, therefore its isotherm was not determined. One hundred milligram samples of SMZ-25, SMZ-50, and SMC-50 were put in contact with 10 mL of different concentrations of DS (0.3, 0.6, 0.9, 1.5, 3.0, 4.5, 6.0, 7.5, 9.0, 10 mg/L). The mixtures were shaken for 48 h at 25˚C and 100 rpm. The clay mixture was centrifuged and the zeolite mixtures were decanted. DS was analyzed in the remaining solutions as described above.

The experimental results were analyzed by nonlinear Langmuir, Freundlich, and Langmuir–Freundlich sorption models with the help of STATISTICA version 7.0 software.

2.7.1. Langmuir model

Langmuir isotherm is based on the following assumptions: the molecules are adsorbed on a certain number of sites located in fixed positions, each adsorption site accepts only a molecule and they are arranged in a monolayer, all sites are energetically equivalent, there are not any lateral interactions between adsorbed molecules, adsorption rate is proportional to the fraction, and free concentration unoccupied adsorption sites. Langmuir model is probably the most widely applied [28].

It may be represented as follows:

$$q_e = qK_L C_e/(1 + K_L C_e) \tag{5}$$

where q (mg/g) is the amount of DS adsorbed per unit weight of adsorbent in forming a complete monolayer on the surface, q_e (mg/g) is the total amount of DS adsorbed per unit weight of adsorbent at equilibrium, C_e (mg/L) is the concentration of the DS in the solution at equilibrium, and K_L is a constant related to the energy or net enthalpy of sorption.

2.7.2. Freundlich model

Freundlich isotherm is an empirical expression involving the heterogeneity of the surface and the exponential distribution of the adsorption sites and energy. The Freundlich empirical model can be applied to a nonideal sorption on heterogeneous surfaces as well as to a multilayer sorption and can be expressed by the following equation [28]:

$$q_e = K_f\, C_e^{1/n} \tag{6}$$

where q_e (mg/g) is the total amount of fluoride ions adsorbed per unit weight of adsorbent at equilibrium, C_e (mg/L) is the concentration of the DS in the solution at equilibrium; K_f is the equilibrium constant indicative of sorption capacity and n is an empirical constant.

2.7.3. Langmuir–Freundlich model

The Langmuir–Freundlich model is a combination of both Langmuir and Freundlich models and it can be expressed by the following equation [28]:

$$q_e = K_{LF} C_e^{1/n}/(1 + a_{LF} C_e^{1/n}) \tag{7}$$

where q_e is the amount of DS per unit weight of material (mg/g), C_e is the equilibrium concentration of DS in solution (mg/L), K_{LF} and a_{LF} are empirical constants.

2.8. Characterization techniques

2.8.1. X-ray diffraction (XRD)

Powder patterns were measured at room temperature on a Siemens D500 diffractometer coupled to a copper anode X-ray tube in the 5°–70° 2θ range, step of 0.070°, step time of 1.6 s, and time started of 11 s. The conventional diffractograms were used to identify the compounds and to verify crystalline structure.

2.8.2. Fourier transform infrared spectroscopy (FT-IR)

The IR spectra in the 4,000–400 cm^{-1} range, resolution of 2.0, and number of scans of 32 were recorded for both adsorbents at room temperature using an AVATAR 360 ESP Nicolet fourier transform infrared spectroscopy (FT-IR) spectrophotometer. The samples were prepared using the standard KBr pellet method.

2.8.3. Scanning Electron Microscopy (SEM)

The surface morphology and the chemical composition of samples were investigated using a JEOL JSM-6510 scanning electron microscope (SEM) equipped with X-ray energy dispersive detector (EDS). Observations were performed with samples coated with gold. EDS elemental analyses were performed on a significantly high number of analysis (15), in order to detect the distribution of the elements on the surfaces.

2.8.4. Thermogravimetric analysis

Thermogravimetric analysis of the unmodified zeolitic tuff and unmodified clay were performed on a TA Instruments SDT Q600. Samples were heated (20–950℃) in a nitrogen atmosphere, at a heating rate of 10℃/min.

3. Results and discussion

3.1. Characterization

3.1.1. Scanning electron microscopy (SEM)

Fig. 1(a) and (b) shows the morphology of the unmodified and HDTMA modified zeolitic tuff, respectively, it can be observed the typical morphology of sedimentary, clinoptilolite-rich tuffs [18] with coffin and cubic-like crystals of the sodium zeolite.

Fig. 1(c) shows the typical morphology of unmodified clay with curved plates either with face-to-edge contacts between particles or covered by small and well-separated particles [29]. Fig. 1(d) shows the morphology of HDTMA modified clay (SMC-50) there are

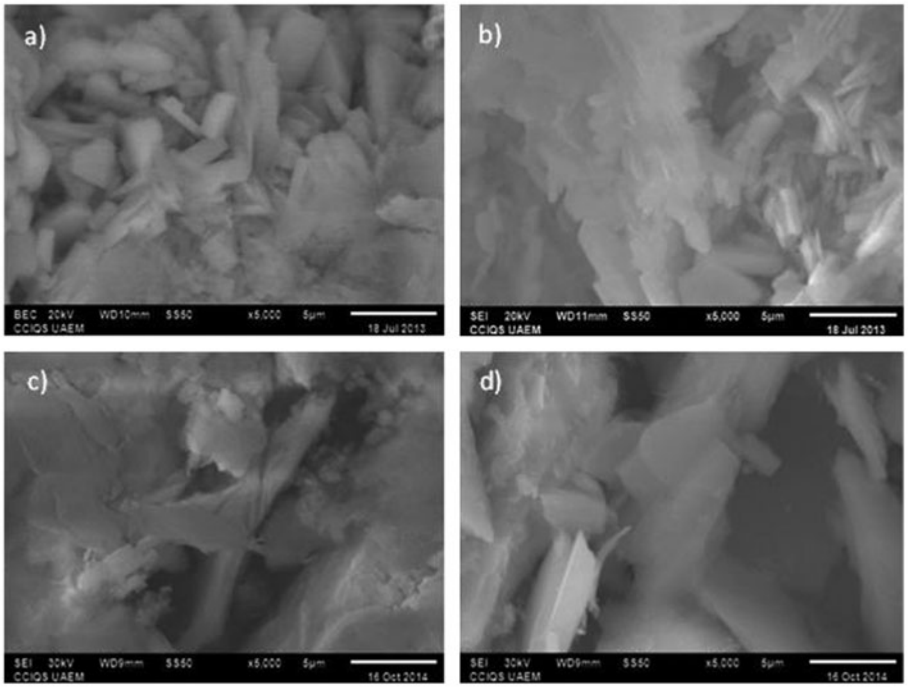

Fig. 1. SEM images of the (a) Z-Na, (b) SMZ-50, (c) C, and (d) SMC-50.

small and aggregated particles on the plates, in comparison to the morphology of unmodified clay. He et al. [30] reported that not only the basal spacing but also the morphology of the HDTMA modified clay depends on the packing density of surfactant within the montmorillonite interlayer space. The structures of grain-type and agglomerates found in SMC-50 show the ability of the particles to form aggregates, which are bigger than that of raw montmorillonite. This feature is due to the surfactants that compensate the negative charge of the particles and, thus, eliminate the repulsive electrostatic forces between them [31].

Churchman [32] reported a montmorillonite charge reversal, by adsorption of quaternary ammonium derivatives of polymers, from a net negative charge at zero loading to a net positive charge as the polycation content increased. This behavior was explained considering the entrance of polycations into the montmorillonite interlayer space and simultaneously, even at very low loadings, considering adsorption of polycations on the external surfaces.

The chemical compositions of the unmodified, sodium and HDTMA modified zeolitic tuff and unmodified clay and HDTMA modified clay are

Table 1
Elemental composition of unmodified and modified zeolitic tuff

Element	Z wt (%)	Z-Na wt (%)	SMZ-25 wt (%)	SMZ-50 wt (%)
N	–	–	21.077 ± 1.052	51.154 ± 1.286
Na	1.174 ± 0.426	2.124 ± 0.401	0.853 ± 0.049	2.407 ± 0.279
Mg	3.030 ± 0.081	2.274 ± 0.176	5.631 ± 0.010	5.975 ± 0.885
Al	9.896 ± 1.179	10.522 ± 1.075	0.987 ± 0.051	1.935 ± 0.133
Si	68.736 ± 2.025	64.729 ± 2.541	40.552 ± 1.545	24.673 ± 2.770
K	9.780 ± 1.652	5.781 ± 1.019	4.637 ± 1.003	1.409 ± 0.536
Ca	10.531 ± 0.219	4.141 ± 1.928	10.081 ± 0.952	3.035 ± 0.181
Ti	0.481 ± 0.090	0.477 ± 0.094	0.309 ± 0.012	0.042 ± 0.003
Fe	5.068 ± 0.191	4.350 ± 1.003	3.562 ± 0.648	1.904 ± 0.317

Table 2
Elemental composition of the unmodified and modified clay

Element	C wt (%)	SMC-25 wt (%)	SMC-50 wt (%)
N	–	22.000 ± 2.443	53.319 ± 0.707
Na	1.052 ± 0.004	–	0.125 ± 0.064
Mg	3.940 ± 0.120	2.011 ± 0.387	2.171 ± 0.395
Al	10.267 ± 1.749	2.434 ± 0.155	1.872 ± 0.794
Si	79.871 ± 2.398	37.183 ± 0.575	56.869 ± 2.398
K	1.444 ± 0.191	–	–
Ca	1.767 ± 0.767	–	0.255 ± 0.080
Ti	1.993 ± 0.231	–	0.127 ± 0.079

presented in Tables 1 and 2, respectively. The main elements are Si and Al corresponding to aluminosilicates. Mg, K, Ca, and Fe content diminished when the materials were treated with NaCl, this behavior indicates that these elements were replaced by Na in the materials. Nitrogen was found in the samples treated with HDTMA.

3.1.2. Thermogravimetric analysis

Thermogravimetric analyses for unmodified and sodium modified zeolitic tuff were performed. The thermogram for unmodified zeolitic tuff (Fig. 2(a)) shows that up to 363˚C there is moisture loss, from 363 to 473˚C dehydration was observed, from 473˚C to 773˚C intra reticular water loss occurred. In the temperature range from 773 to 873˚C, slower rate loss related to decomposition of the sample was observed. The total weight loss was 16.55% for the unmodified material. The thermogram for sodium zeolitic tuff (Fig. 2(b)) shows the maximum weight loss was 9.76% and the principal loss was observed between 293 and 623˚C, so it could be attributed to loss of bounded water in the zeolite structure [33] with a continuous weight loss up to 950˚C.

The thermogram for unmodified clay (Fig. 2(c)) shows two endothermic reactions, the first at 300˚C, with a loss of 6.88% of weight, due to the water adsorbed on clay surface. The second reaction occurs between 300 and 950˚C, with a weight loss of 3.98% caused by the removal of water from interlaminar spaces. The total weight loss was 10.86% at almost 950˚C.

3.1.3. X-ray diffraction (XRD)

The X-ray Diffraction (XRD) patterns of the unmodified and sodium modified zeolitic tuff are shown in Fig. 3(a) and (b). The diffractograms were compared with clinoptilolite (JCPDS 039-1383), quartz (JCPDS 01–085-0865) and albite (JCPDS 01–072-1246) which were the principal components found in the zeolitic tuff samples. These results suggested there were not any notable changes in structure of clinoptilolite after it was treated with NaCl.

The X-ray powder diffraction pattern of the unmodified clay is shown in Fig. 3(c). The diffractogram was compared with monmorillonite (JCPDS 03–03-0015), quartz (JCPDS 03–065-0466), cristobalite (JCPDS 01–077-1316), and albite (JCPDS 01–072-1246) which were the principal components found in the clay samples.

3.1.4. Fourier transform infrared spectroscopy (FT-IR)

The FT-IR spectra of the Z-Na and SMZ-50 are shown in Fig. 4(a). The most intense band is observed at 1,047 cm^{-1}, which is due to external tetrahedral linkage asymmetric stretching. The position of this band is very sensitive to the number of Al atoms in the zeolite [34].

The spectra display three intense bands at 1,638, 3,437, and 3,619 cm^{-1}; they can be assigned to OH^- stretching vibration mode of adsorbed water in the zeolite, intermolecular hydrogen bonding, and Si–OH–Al bridges [34].

Comparing the FT-IR spectra of the Z-Na and SMZ-50, two new bands appear around 2,950 and 2,850 cm^{-1}, which could be attributed to the presence of HDTMA on the zeolite surface. The bands have been attributed to asymmetric and symmetric stretching vibrations of C–H of the methylene groups, respectively [35].

The FT-IR spectra for the unmodified clay and SMC-50 are shown in Fig. 4(b). All samples revealed a band at 1,030 cm^{-1}, assigned to from Si–O stretching vibrations. There were bands characteristic of water molecules (1,630–1,650 cm^{-1}). The bands at

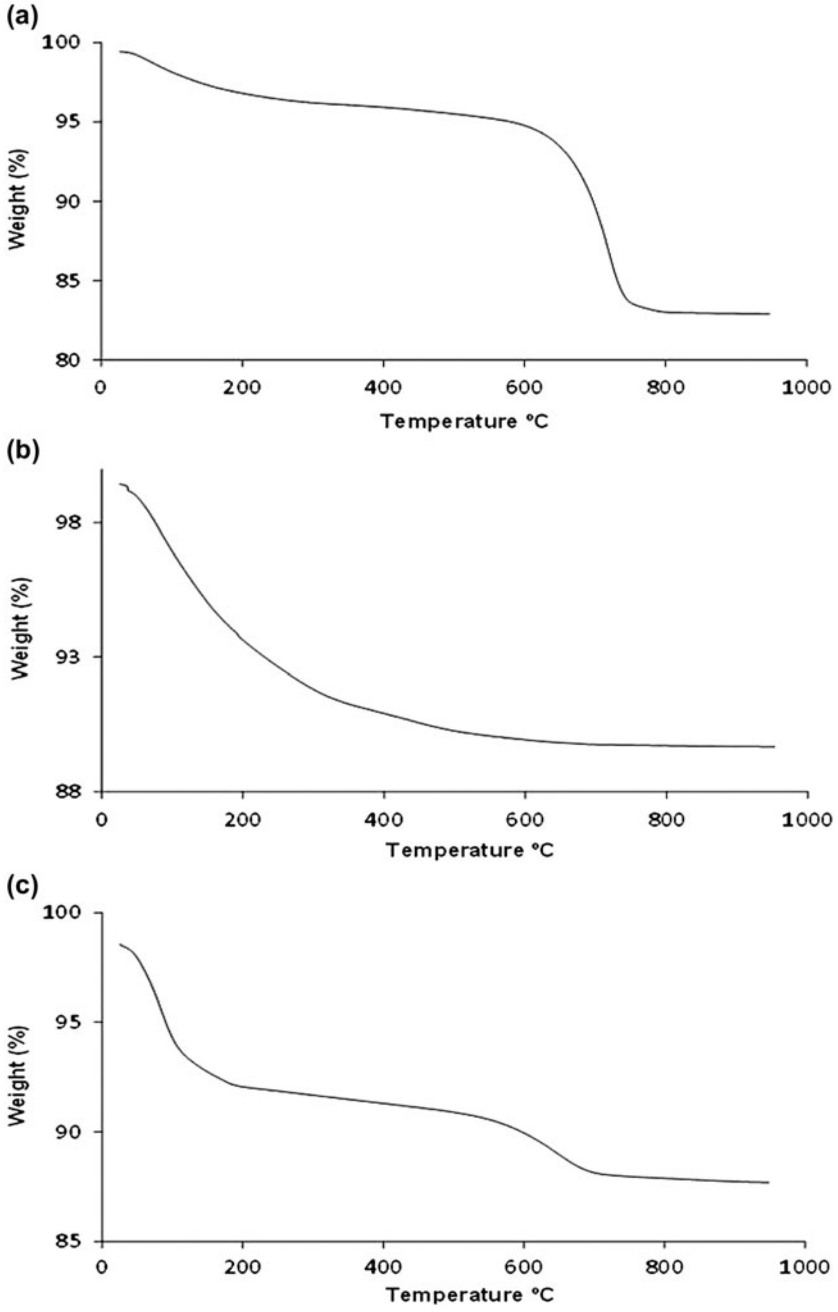

Fig. 2. Thermogram for (a) unmodified zeolitic, (b) sodium modified zeolitic, and (c) unmodified clay.

3,620–3,696 cm^{-1}, corresponded to O–H stretching vibrations, bands at 1,470–1,472 cm^{-1}, result from HDTMA methyl group vibrations. According to Gladysz-Plaska et al. [36] bands at (2,800–3,000 cm^{-1}) have been attributed to symmetric and asymmetric stretching vibrations of C–H bonds of the surfactant methylene groups.

3.1.5. Zero charge point determination

The zero charge points for the unmodified and HDTMA modified zeolitic tuff were determined when the equilibrium pH values were equal or quite similar to the initial pH; they were 7.0, 8.1, and 8.6 for the unmodified zeolitic tuff, SMZ-25, and SMZ-50, respectively.

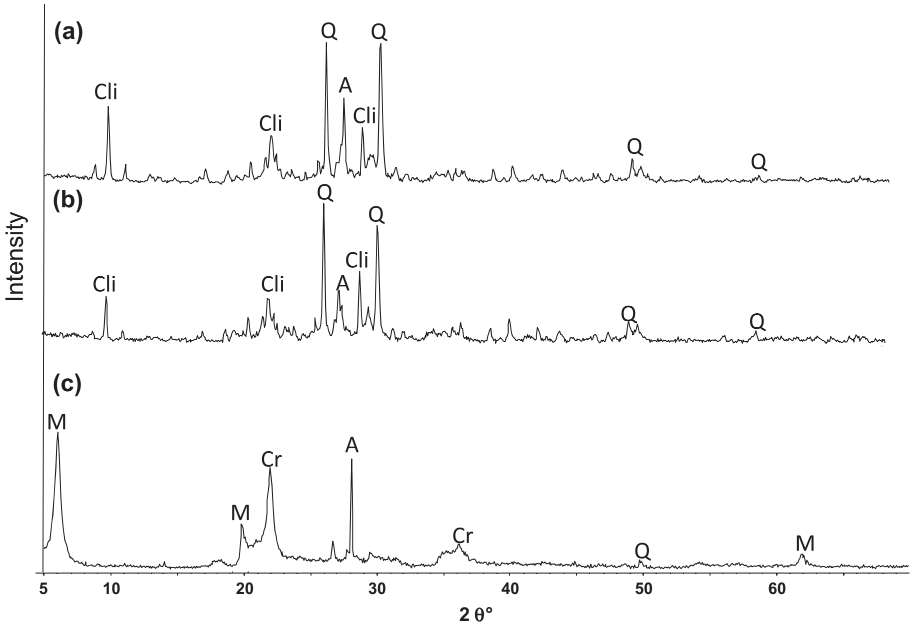

Fig. 3. X-ray powder diffraction pattern the (a) unmodified zeolitic, (b) sodium modified zeolitic, and (c) unmodified clay.

Notes: Montmorillonite JCPDS 03–03-0015 (M), Cristobalite JCPDS 01–077-1316 (Cr), Albite JCPDS 01–072-1246 (A), Quartz JCPDS 03–065-0466 (Q), Clinoptilolite JCPDS 039-1383 (Cli).

The zero charge points for the unmodified and HDTMA modified clays were 8.1, 7.5, and 7.4 for the unmodified clay, SMZ-25, and SMZ-50, respectively

3.2. Sorption kinetics

Fig. 5(a) shows the relationship between contact time and the sorption capacities of unmodified zeolitic, and HDTMA (25 and 50 mM) modified zeolitic tuff. It is important to note that the unmodified material does not adsorb any quantity of solute, due to the hydrophilic and hydrophobic characteristics of the sodium zeolitic tuff and the solute. According to the figure, equilibrium was reached in about 44 h for both HDTMA modified materials. It was observed as well that the adsorption rates were similar for both modified zeolitic tuff samples. The initial pHs were 6.5 for both SMZ-25 and SMZ-50.

The kinetic parameters were calculated by applying pseudo-first-order, pseudo-second-order and Elovich models but the standard deviations of the experiments were high as shown in Fig. 5(a) although the best adjusted was to the pseudo-second-order model because the capacities calculated and obtained experimentally were similar, which may indicate that the sorption process is chemisorption.

Fig. 5(b) shows the relationships between contact time and the sorption capacities of unmodified clay, and HDTMA (25–50 mM) modified clays. It is important to note that the unmodified material did not adsorb any quantity of solute, due to the hydrophilic and hydrophobic characteristics of the unmodified clay and the solute.

According to this figure, equilibrium was reached in about 24 h for SMC-25 and about 28 h for SMC-50 with initial pH values of 6.2 and 6.5, respectively. The sorption capacities were of 0.436 ± 0.015 and 0.880 ± 0.012 for SMC-25 and SMC-50, respectively. The kinetic parameters were calculated by applying pseudo-first-order, pseudo-second-order and Elovich models to the experimental results.

Table 3 shows the parameters calculated by each model. The experimental data of SMC-50 were best adjusted to the pseudo-second-order model because the adsorption capacities calculated and experimentally obtained were similar.

3.3. Sorption isotherms

Fig. 6(a) shows the isotherms experimental data for DS sorption by SMZ-25 and SMZ-50. The sorption capacities for both materials (SMZ-25 and SMZ-50) are of the same order of magnitude (0.826 ± 0.004 and 0.821 ± 0.002, respectively), considering the low concentrations of DS found in wastewaters [6], these materials may be used to remove this drug. Table 4

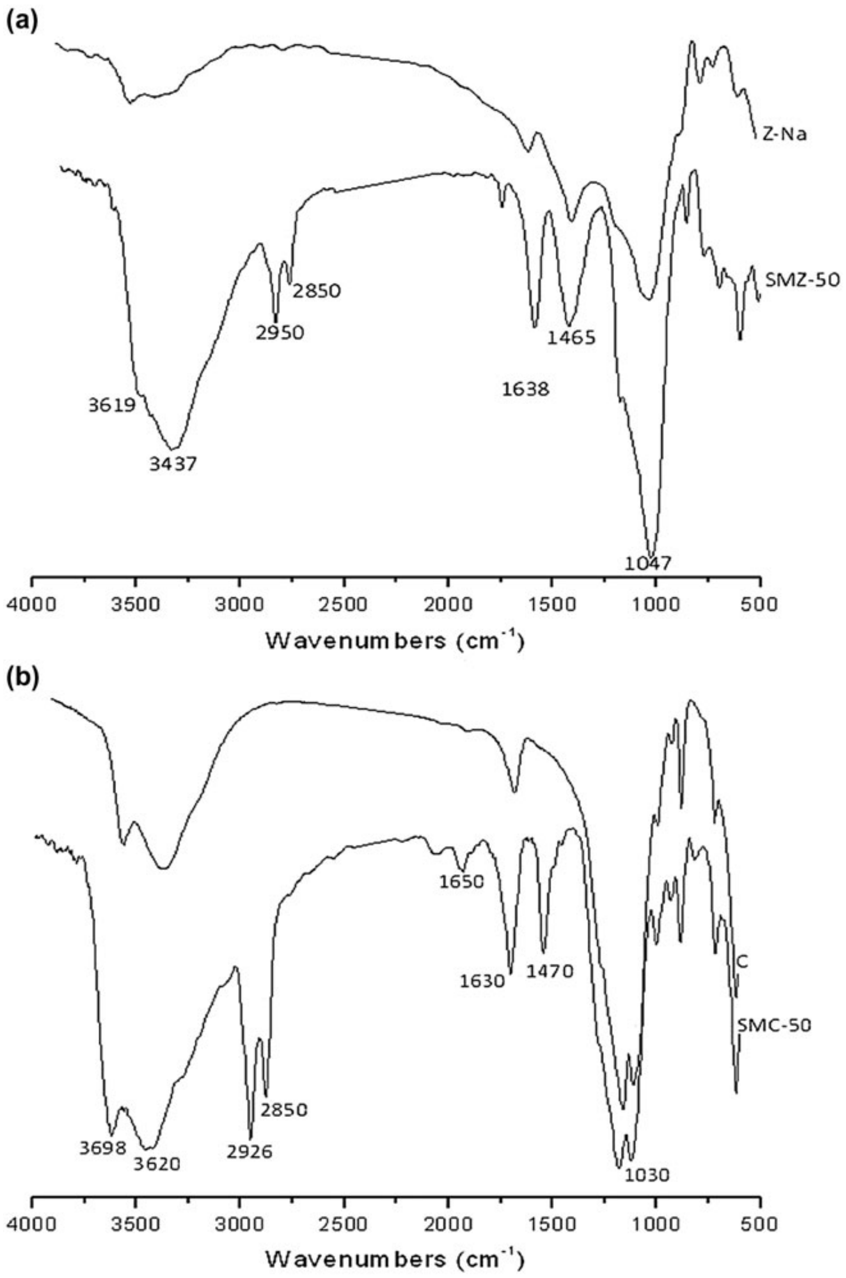

Fig. 4. FT-IR spectrum for (a) Z-Na and SMZ-50, (b) unmodified clay, and (C) SMC-50.

shows the isotherm parameters of the DS sorption by SMZ-25 and SMZ-50, the experimental data were best adjusted to the Langmuir model indicating that the material is homogeneous. SMZ-25 showed a higher sorption capacity than SMZ-50 probably due to the excess of surfactant in the sample that may form micelles on the surface of the material [21]. According to the kinetic and isotherm results, the SMZ-25 showed the best properties for DS removal from aqueous solutions.

According to Krajišnik et al. [21], the sorption of DS is assumed to take place at the hydrophobic phase created by surfactant tail groups on the zeolitic surface because it is a hydrophobic organic molecule.

The equilibrium isotherms for SMC-50 is presented in Fig. 6(b), as it observed the experimental data follow a liner equation which is characteristic for sorption of organic solutes by the partition mechanism described elsewhere [37]. The partitioning effect may

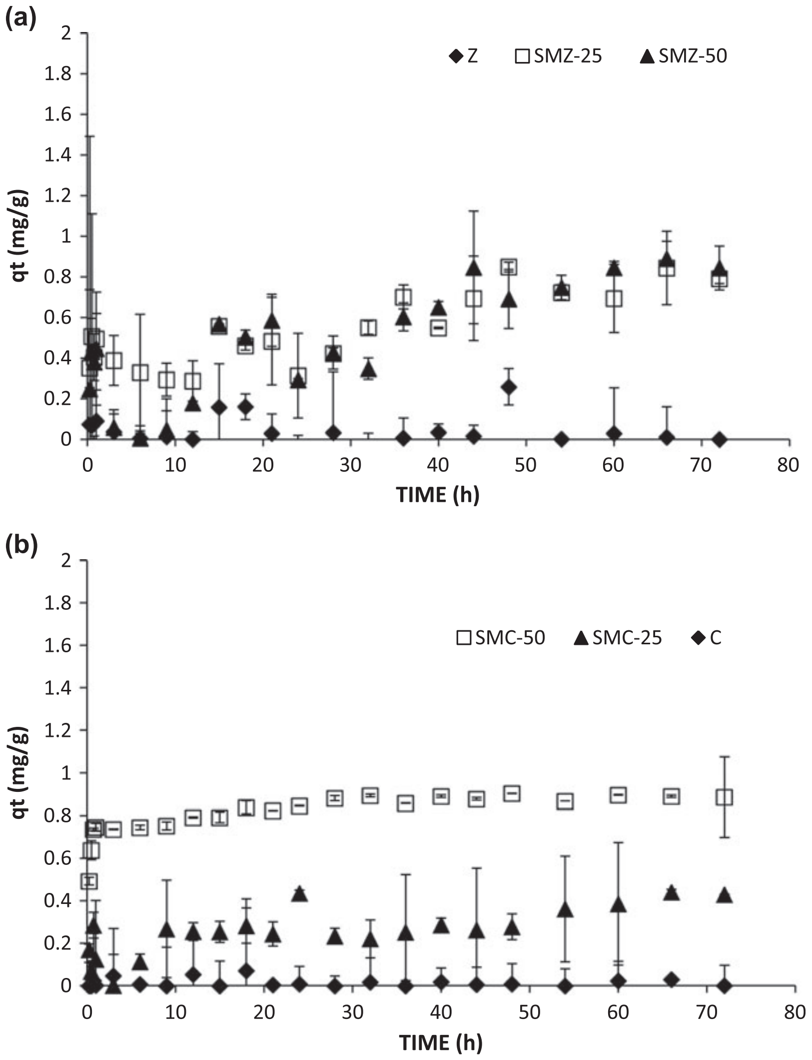

Fig. 5. Adsorption of diclofenac (DS) (a) unmodified zeolitic (Z) SMZ-25 and SMZ-50, (b) unmodified clay, and (C) SMC-25 and SMC-50.

Table 3
Kinetic parameters of the DS sorption by the modified clay with 25–50 mM of HDTMA

	Lagergren $q_t = q_e^{(1-\exp(-K_L t))}$			Ho $q_t = Kq_e^2 t/(1 + Kq_e t)$			Elovich $q_t = \beta \ln \alpha + \beta \ln t$		
Sample	K_L (h^{-1})	q_e (mg/g)	r^2	K (g/mg h)	q_e (mg/g)	r^2	α (mg/g h)	β (mg/g)	r^2
SMC-25	1.350	0.016	0.200	177.165	0.016	0.161	–	–	–
SMC-50	2.805	0.839	0.872	5.209	0.895	0.973	17147.042	0.200	0.939

be attributed to the long alkyl chains of the quaternary ammonium cations and it is favored by interlayer expansion [19]. The equation for sorption of DS is $q_e = 0.5914\ C_e$ and R^2 of 0.8789. The slope corresponds to the distribution coefficient (K_d) which indicates the partition of the solute between the adsorbent and solution.

According to Sheng et al. [37], there are two types of interactions between polar organic compounds and modified clays, i.e. adsorption and partition (modified bentonites with small quaternary ammonium cations exhibit mainly adsorption, while modified bentonites with large alkyl groups display mainly partition), linear adsorption isotherm is characteristics of partition.

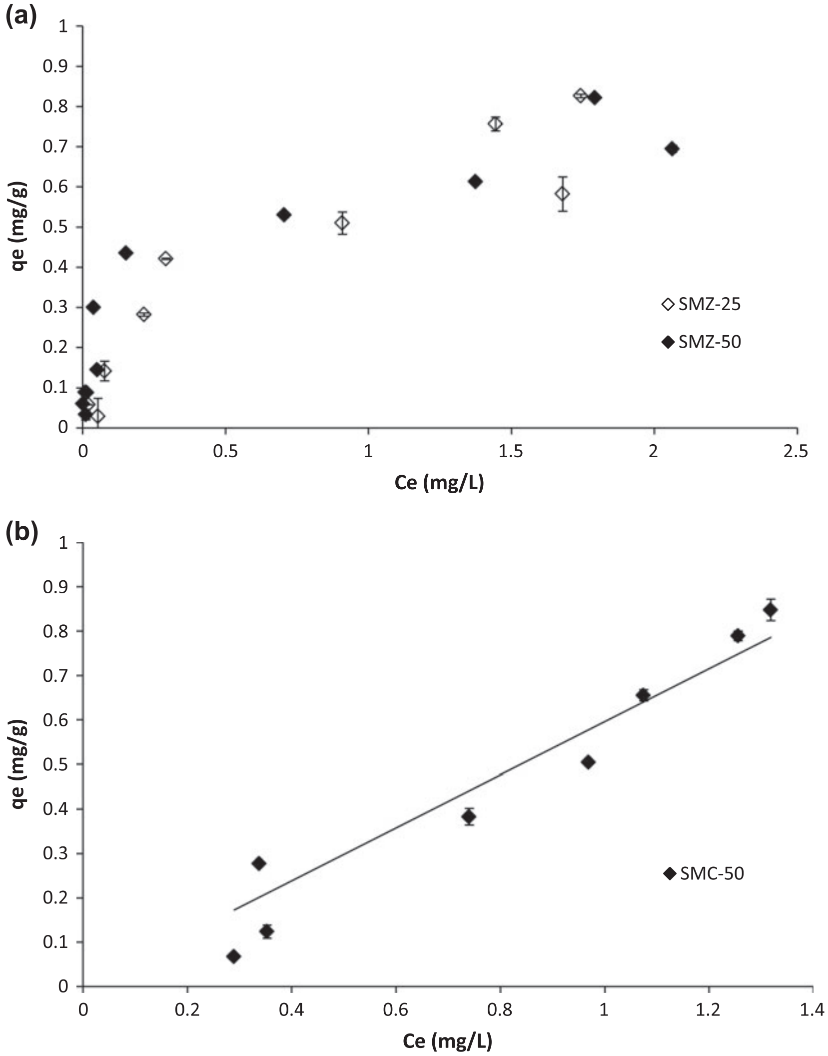

Fig. 6. Isotherm DS (a) SMZ-25 and SMZ-50 and (b) SMC-50.

Table 4
Isotherm parameters of the diclofenac sorption by the SMZ-25 and SMZ-50

	Langmuir $q_e = q_m K_L C_e/(1 + K_L\ C_e)$				Freundlich $q_e = K_F {C_e}^{1/n}$		Langmuir–Freundlich $q_e = K_{LF} {C_e}^{1/n}/(1 + a_{LF} {C_e}^{1/n})$			
Sample	K_L (L/g)	q_m (mg/g)	r^2	K_F (L/g)	$1/n$	r^2	K_{LF}	a_{LF}	$1/n$	r^2
SMZ-25	2.249	0.897	0.963	0.467	0.002	0.869	0.238	0.265	2.137	0.963
SMZ-50	8.638	0.732	0.961	0.425	0.002	0.742	–	–	–	–

Adsorption/partition mechanisms have been reported for nonlinear isotherms for sorption of phenol, p-chlorophenol and 2,4-dichlorophenol by modified HDTMA bentonite [38] at low concentrations is mainly by adsorption at higher concentrations by partition. The sorption behavior depends mainly on the solute properties (water solubility and polarity).

In general, the points of zero charge were 8.1–8.6 and 7.4–7.5 for the HDTMA modified zeolitic tuff and clay, the surface of these materials is positively charged at the studied pH conditions. Hence, it is expected that the electrical charge of DS plays an important role on their adsorption onto modified materials. The pka of DS is 4.18 then the dominant ionized species are anionic at pH higher than 4.18 [22]. The adsorption of these anionic species would be favored on modified zeolitic tuff an clays surfaces positively charged due to electrostatic attraction at pH values between 4.18 and their points of zero charge. In contrast, bilayer formation of HDTMA at the zeolitic tuff and clay surface provides the adsorption sites for DS.

4. Conclusions

Two aluminosilicates were modified with HDTMA and characterized before and after adsorption of DS by different techniques. The adsorption processes of DS by HDTMA modified materials followed the pseudo-second-order kinetic model indicating a chemisorption mechanism. The adsorption capacities determined were of the same order of magnitude for both SMZ-25 and SMZ-50 materials and the equilibrium data over the entire concentration range studied were fitted to the Langmuir equation, indicating that the modified materials are homogeneous. SMC-50 follows a liner isotherm equation which is characteristic for sorption of organic solutes by the partition mechanism. According to the kinetic and isotherm results, SMZ-25 and SMC-50 showed the best properties for DS removal from aqueous solutions. The adsorption capacities of these materials and the low concentrations of DS in wastewaters show these materials are potential adsorbents to remove this drug.

Acknowledgments

This work was done under the CONACYT project 215997 and CONACYT for the grant number 231507 to P.A.G.

References

[1] W.J. Sim, J.W. Lee, E.S. Lee, S.K. Shin, S.R. Hwang, J.E. Oh, Occurrence and distribution of pharmaceuticals in wastewater from households, livestock farms, hospitals and pharmaceutical manufactures, Chemosphere 82 (2011) 179–186.

[2] K.H. Langford, K.V. Thomas, Determination of pharmaceutical compounds in hospital effluents and their contribution to wastewater treatment works, Environ. Int. 35 (2009) 766–770.

[3] T. Kosjek, E. Heath, A. krbavčič, Determination of non-steroidal anti-inflammatory drug (NSAIDs) residues in water samples, Environ. Int. 31 (2005) 679–685.

[4] Y. Zhang, S.U. Geißen, C. Gal, Carbamazepine and diclofenac: Removal in wastewater treatment plants and occurrence in water bodies, Chemosphere 73 (2008) 1151–1161.

[5] N. Suriyanon, P. Punyapalakul, C. Ngamcharussrivichai, Mechanistic study of diclofenac and carbamazepine adsorption on functionalized silica-based porous materials, Chem. Eng. J. 214 (2013) 208–218.

[6] M.J. Gómez, A. Agüera, M. Mezcua, J. Hurtado, F. Mocholí, A.R. Fernández-Alba, Simultaneous analysis of neutral and acidic pharmaceuticals as well as related compounds by gas chromatography-tandem mass spectrometry in wastewater, Talanta 73 (2007) 314–320.

[7] B. Ferrari, N. Paxéus, R. Lo Giudice, A. Pollio, J. Garric, Ecotoxicological impact of pharmaceuticals found in treated wastewaters: Study of carbamazepine, clofibric acid, and diclofenac, Ecotoxicol. Environ. Saf. 55 (2003) 359–370.

[8] E.J. van den Brandhof, M. Montforts, Fish embryo toxicity of carbamazepine, diclofenac and metoprolol. Ecotoxicol. Environ. Saf. 73 (2010) 1862–1866.

[9] J. Schwaiger, H. Ferling, U. Mallow, H. Wintermayr, R.D. Negele, Toxic effects of the non-steroidal anti-inflammatory drug diclofenac. Part I: Histopathological alterations and bioaccumulation in rainbow trout, Aquat. Toxicol. 68 (2004) 141–150.

[10] H.S. Chang, K.H. Choo, B. Lee, S.J. Choi, The methods of identification, analysis, and removal of endocrine disrupting compounds (EDCs) in water, J. Hazard. Mater. 172 (2009) 1–12.

[11] A.M. Urtiaga, G. Pérez, R. Ibáñez, I. Ortiz, Removal of pharmaceuticals from a WWTP secondary effluent by ultrafiltration/reverse osmosis followed by electrochemical oxidation of the RO concentrate, Desalination 331 (2013) 26–34.

[12] T.A. Ternes, J. Stüber, N. Herrmann, D. McDowell, A. Ried, M. Kampmann, B. Teiser, Ozonation: A tool for removal of pharmaceuticals, contrast media and musk fragrances from wastewater? Water Res. 37 (2003) 1976–1982.

[13] D.P. Mohapatra, S.K. Brar, R.D. Tyagi, P. Picard, R.Y. Surampalli, Analysis and advanced oxidation treatment of a persistent pharmaceutical compound in wastewater and wastewater sludge-carbamazepine, Sci. Total Environ. 470–471 (2014) 58–75.

[14] N. Tran, P. Drogui, F. Zaviska, S.K. Brar, Sonochemical degradation of the persistent pharmaceutical carbamazepine, J. Environ. Manage. 131 (2013) 25–32.

[15] I. Braschi, S. Blasioli, L. Gigli, C.E. Gessa, A. Alberti, A. Martucci, Removal of sulfonamide antibiotics from water: Evidence of adsorption into an organophilic zeolite Y by its structural modifications, J. Hazard. Mater. 178 (2010) 218–225.

[16] S. Fukahori, T. Fujiwara, R. Ito, N. Funamizu, pH-dependent adsorption of sulfa drugs on high silica zeolite: Modeling and kinetic study, Desalination 275 (2011) 237–242.

[17] R.S. Bowman, Applications of surfactant-modified zeolites to environmental remediation, Microporous Mesoporous Mater. 61 (2003) 43–56.

[18] F.A. Mumpton, W.C. 0rsmy, Morphology of zeolites in sedimentary rocks by scanning electron microscopy, Clays Clay Miner. 24 (1976) 1–23.

[19] H.A. Patel, H.C. Bajaj, R.V. Jasra, Sorption of nitrobenzene from aqueous solution on organoclays in batch and fixed-bed systems, Ind. Eng. Chem. Res. 48 (2009) 1051–1058.

[20] A.Z. Redding, S.E. Burns, R.T. Upson, E.F. Anderson, Organoclay sorption of benzene as a function of total organic carbon content, J. Colloid Interface Sci. 250 (2002) 261–264.

[21] D. Krajišnik, A. Daković, M. Milojević, A. Malenović, M. Kragović, D.B. Bogdanović, Properties of diclofenac sodium sorption onto natural zeolite modified with cetylpyridinium chloride, Colloids Surf. B 83 (2011) 165–172.

[22] T.X. Bui, S.Y. Kang, S.H. Lee, H. Choi, Organically functionalized mesoporous SBA-15 as sorbents for removal of selected pharmaceuticals from water, J. Hazard. Mater. 193 (2011) 156–163.

[23] C. Díaz-Nava, M.T. Olguín, M. Solache-Ríos, M.T. Alarcón-Herrera, A. Aguilar-Elguezabal, Phenol sorption on surfactant-modified Mexican zeolitic-rich tuff in batch and continuous systems, J. Hazard. Mater. 167 (2009) 1063–1069.

[24] A. Teutli-Sequeira, M. Solache-Ríos, V. Martínez-Miranda, I. Linares-Hernández, Comparison of aluminum modified natural materials in the removal of fluoride ions, J. Colloid Interface Sci. 418 (2014) 254–260.

[25] M.J. Jiménez-Cedillo, M.T. Olguín, Ch. Fall, Adsorption kinetic of arsenates as water pollutant on iron, manganese and iron–manganese-modified clinoptilolite-rich tuffs, J. Hazard. Mater. 163 (2009) 939–945.

[26] Y.S. Ho, Review of second-order models for adsorption systems, J. Hazard. Mater. 136 (2006) 681–689.

[27] Y.S. Ho, G. McKay, A comparison of chemisorption kinetic models applied to pollutant removal on various sorbents, Process Saf. Environ. Prot. 76 (1998) 332–340.

[28] A.B. Pérez-Marín, V.M. Zapata, J.F. Ortuño, M. Aguilar, J. Sáez, M. Lloréns, Removal of cadmium from aqueous solutions by adsorption onto orange waste, J. Hazard. Mater. 139 (2007) 122–131.

[29] A.E. Bianchi, M. Fernández, M. Pantanetti, R. Viña, I. Torriani, R.M.T. Sánchez, $ODTMA^+$ and $HDTMA^+$ organo-montmorillonites characterization: New insight by WAXS, SAXS and surface charge, Appl. Clay Sci. 83–84 (2013) 280–285.

[30] H. He, R.L. Frost, T. Bostrom, P. Yuan, L. Duong, D. Yang, Changes in the morphology of organoclays with $HDTMA^+$ surfactant loading, Appl. Clay Sci. 31 (2006) 262–271.

[31] M. Pospíšil, P. Čapková, D. Měřínská, Z. Maláč, J. Šimoník, Structure analysis of montmorillonite intercalated with cetylpyridinium and cetyltrimethylammonium: Molecular simulations and XRD analysis, J. Colloid Interface Sci. 236 (2001) 127–131.

[32] G.J. Churchman, Formation of complexes between bentonite and different cationic polyelectrolytes and their use as sorbents for non-ionic and anionic pollutants, Appl. Clay Sci. 21 (2002) 177–189.

[33] A. Martucci, L. Pasti, N. Marchetti, A. Cavazzini, F. Dondi, A. Alberti, Adsorption of pharmaceuticals from aqueous solutions on synthetic zeolites, Microporous Mesoporous Mater. 148 (2012) 174–183.

[34] K. Elaiopoulos, T. Perraki, E. Grigoropoulou, Mineralogical study and porosimetry measurements of zeolites from Scaloma area, Thrace, Microporous Mesoporous Mater. 112 (2008) 441–449.

[35] D. Bhardwaj, M. Sharma, P. Sharma, R. Tomar, Synthesis and surfactant modification of clinoptilolite and montmorillonite for the removal of nitrate and preparation of slow release nitrogen fertilizer, J. Hazard. Mater. 227–228 (2012) 292–300.

[36] A. Gładysz-Płaska, M. Majdan, S. Pikus, D. Sternik, Simultaneous adsorption of chromium(VI) and phenol on natural red clay modified by HDTMA, Chem. Eng. J. 179 (2012) 140–150.

[37] G. Sheng, S. Xu, S.A. Boyd, Cosorption of organic contaminants from water by hexadecyltrimethylammonium-exchanged clays, Water Res. 30 (1996) 1483–1489.

[38] Z. Rawajfih, N. Nsour, Characteristics of phenol and chlorinated phenols sorption onto surfactant-modified bentonite, J. Colloid Interface Sci. 298 (2006) 39–49.